Cell

# Rescue of ΔF508-CFTR Trafficking via a GRASP-Dependent Unconventional Secretion Pathway

Heon Yung Gee,[1,3] Shin Hye Noh,[1,3] Bor Luen Tang,[2] Kyung Hwan Kim,[1] and Min Goo Lee[1,*]
[1]Department of Pharmacology, Brain Korea 21 Project for Medical Sciences, Severance Biomedical Science Institute, Yonsei University College of Medicine, Seoul 120-752, Korea
[2]Department of Biochemistry, Yong Loo Lin School of Medicine, National University of Singapore, 117597 Singapore
[3]These two authors equally contributed to this work
*Correspondence: mlee@yuhs.ac
DOI 10.1016/j.cell.2011.07.021

## SUMMARY

The most prevalent disease-causing mutation of CFTR is the deletion of Phe508 (ΔF508), which leads to defects in conventional Golgi-mediated exocytosis and cell surface expression. We report that ΔF508-CFTR surface expression can be rescued in vitro and in vivo by directing it to an unconventional GRASP-dependent secretion pathway. An integrated molecular and physiological analysis indicates that mechanisms associated with ER stress induce cell surface trafficking of the ER core-glycosylated wild-type and ΔF508-CFTR via the GRASP-dependent pathway. Phosphorylation of a specific site of GRASP and the PDZ-based interaction between GRASP and CFTR are critical for this unconventional surface trafficking. Remarkably, transgenic expression of GRASP in ΔF508-CFTR mice restores CFTR function and rescues mouse survival without apparent toxicity. These findings provide insight into how unconventional protein secretion is activated, and offer a potential therapeutic strategy for the treatment of cystic fibrosis and perhaps diseases stemming from other misfolded proteins.

## INTRODUCTION

The cystic fibrosis transmembrane conductance regulator (CFTR) is a cAMP-activated anion channel responsible for transepithelial chloride and bicarbonate transport in the airway, exocrine pancreas, intestine, and genitourinary systems (Park et al., 2010; Quinton, 1999). CFTR also regulates other ion channels and transporters in these epithelia and functions as a central regulator and mediator of fluid and ion secretion (Kunzelmann, 2001; Lee et al., 2007). Consequently, loss of CFTR function resulting from gene mutations underlies a range of epithelial disorders including the classical form of cystic fibrosis (CF), chronic pancreatitis, and infertility in males (see the Cystic Fibrosis Mutation Database, http://www.genet.sickkids.on.ca/app/). CFTR is a glycoprotein that undergoes complex glycosylation as it passes through the Golgi-mediated conventional exocytosis (Quinton, 1999; Ward et al., 1995). Therefore, the fully glycosylated mature CFTR, also known as band C, is expressed at the apical membrane of epithelial tissues (Amaral, 2004). The most common mutation of CFTR, deletion of phenylalanine at position 508 (ΔF508) results in protein misfolding, retention in the endoplasmic reticulum (ER), and finally degradation by the ER-associated degradation (ERAD) pathway (Ward et al., 1995). As a result, negligible amounts of ΔF508-CFTR reach the plasma membrane, and ΔF508-CFTR remains in the ER core-glycosylated immature form, also known as band B, in cells (Amaral, 2004).

Importantly, ΔF508-CFTR can function as a $Cl^-$ channel once it reaches the cell surface (Denning et al., 1992; Namkung et al., 2005). Therefore, many pharmacological and molecular efforts are invested in approaches to facilitate the membrane targeting of ΔF508-CFTR (Becq, 2010). The efficacy of potential ΔF508-CFTR correctors is often evaluated by their ability to enhance the accumulation of band C (Roxo-Rosa et al., 2006), because it is commonly assumed that the complex-glycosylated CFTR is the only form expressed in the plasma membrane. However, notably, recent studies (Luo et al., 2009; Rennolds et al., 2008) and exploratory experiments presented here (Figure S1A available online) suggest that the core-glycosylated CFTR (band B) can also reach the plasma membrane under certain conditions. The trafficking pathways and molecular mechanisms associated with this unconventionally traveled CFTR remain obscure.

The Golgi reassembly stacking proteins (GRASPs) were identified as factors required for the stacking of Golgi cisternae through in vitro assays (Barr et al., 1997). Two isoforms of GRASP, GRASP55 and GRASP65, have been found in vertebrates (Shorter et al., 1999), but their precise physiological role remains elusive. GRASPs are largely dispensable for the conventional anterograde protein transport (Schotman et al., 2008). Interestingly, results from recent studies indicate that GRASPs are involved in the unconventional secretion of proteins that bypasses the Golgi in invertebrate models, although GRASPs were initially known as Golgi-associated proteins. The GRASP homologs in *Dictyostelium* and *Drosophila* mediate the transport of acyl-coenzyme A-binding protein (AcbA) and α-integrin, respectively, at specific developmental stages via

an unconventional Golgi-independent route (Kinseth et al., 2007; Schotman et al., 2008). However, the signaling mechanisms that activate this GRASP-dependent unconventional secretion are largely unknown.

The unfolded protein response (UPR) is an intracellular signaling pathway that is activated by the accumulation of unfolded proteins in the ER (Wiseman et al., 2010). In the ER, secretory and transmembrane proteins fold into their native conformation and undergo posttranslational modifications important for their activity and structure (Schröder and Kaufman, 2005). Perturbations in ER folding capacity by the excessive influx of nascent, unfolded polypeptides activate signaling cascades in the cytosol via transmembrane sensor proteins in the ER membrane. Currently, three arms of the ER stress signaling, namely the inositol-requiring protein 1 (IRE1)-, PKR-like ER localized eIF2$\alpha$ kinase (PERK)-, and activating transcription factor 6 (ATF6)-mediated pathways, are known to mediate the UPR (Schröder and Kaufman, 2005; Wiseman et al., 2010).

In the present study, we report a molecular mechanism whereby ER stress-associated signals and GRASPs play critical roles in the unconventional surface transport of core-glycosylated wild-type (WT) and ΔF508 CFTRs. The selective activation of this unconventional trafficking pathway would be a potential therapeutic strategy for the treatment of diseases arising from conformational changes and transport defects of misfolded proteins.

## RESULTS

### Immature Core-Glycosylated CFTR Can Reach the Plasma Membrane and Are Functional at the Cell Surface

It has been suggested that reducing the incubation temperature (27°C) or treatment with the ER $Ca^{2+}$-ATPase inhibitor thapsigargin can induce the surface expression of ΔF508-CFTR, mainly by disrupting the function of ER quality control system (Denning et al., 1992; Egan et al., 2002). We noted that these maneuvers increased cell surface expression of core-glycosylated CFTR (band B) as well as complex-glycosylated CFTR (band C) (Figure S1A). Therefore, in the first part of the present work, we searched for the molecular mechanism mediating this unusual CFTR trafficking to the plasma membrane.

To determine whether the ER form of CFTR can travel to the cell surface, we blocked the conventional Golgi-mediated exocytic pathway in HEK293 cells expressing WT and ΔF508 CFTR (Figure 1). Inhibition of the anterograde coat protein complex II (COPII)-mediated ER-to-Golgi trafficking was achieved by expression of the dominant-negative form of Sar1, a critical component of the COPII complex (Russell and Stagg, 2010) (Figure 1A). Although the GDP-restricted Sar1-T39N mutant completely blocked the maturation of WT-CFTR glycosylation, the core-glycosylated WT-CFTR was still targeted to the cell surface. Of note, ΔF508-CFTR, which did not travel to cell surface in mock or WT-Sar1 transfected cells, reached the cell surface when ER-to-Golgi trafficking was blocked by the dominant-negative Sar1 mutant (Figure 1A).

The same findings were recapitulated when the conventional ER-to-Golgi trafficking route was blocked by the dominant-negative Arf1-Q71L mutant (Figure 1B) or by syntaxin 5 (STX5) overexpression (Figure 1C). Arf1 is a component of the COPI complex. Although COPI principally mediates retrograde transport from pre-Golgi and Golgi membranes to the ER, it also affects the anterograde transport of vesiculotubular elements from the ER to Golgi stacks (Yoo et al., 2002). STX5 is a target soluble *N*-ethylmaleimide (NEM)-sensitive factor attachment protein receptor (t-SNARE), which is specifically required for the fusion of COPII transport vesicles with acceptor Golgi membranes (Hong, 2005). Overexpression of STX5 inhibited ER-to-Golgi traffic by disrupting the stoichiometric balance of functional SNARE complexes (Gee et al., 2010; Yoo et al., 2002). As shown in Figure 1C, overexpression of STX5, but not STX13 (which is involved in endosome recycling), blocks maturation of CFTR complex-glycosylation. The results in Figure 1D show that membrane trafficking of the human transferrin receptor 1, a type II membrane glycoprotein, is almost completely blocked by the Sar1 and Arf1 mutants and by STX5 overexpression, indicating that conventional ER-to-Golgi transport is indeed blocked by expression of these proteins in HEK293 cells. Furthermore, surface expressed WT and ΔF508 CFTRs in cells expressing the mutant Arf1-Q71L are endoglycosidase H-sensitive (Figure 1E), which corroborates the notion that surface expressed CFTRs are only ER core-glycosylated and a Golgi-independent route mediates their surface trafficking. Lastly, treatment with brefeldin A, a fungal metabolite that induces a block in ER-to-Golgi transport and collapse of the Golgi stacks by inhibiting the function of Arf (Helms and Rothman, 1992), also permitted and enhanced the surface expression of core-glycosylated WT and ΔF508 CFTRs (Figures S1B and S1C). Therefore, when ER-to-Golgi trafficking is blocked by various conditions, the core-glycosylated WT and ΔF508 CFTRs can nonetheless reach the plasma membrane.

To further substantiate our observation of targeting of core-glycosylated CFTR to the plasma membrane, we evaluated the surface expression of CFTR by a surface enzyme-linked immunosorbent assay (ELISA) using extracellular HA epitope-tagged CFTR constructs. As shown in Figure S2, results from cell surface ELISA confirm the biotinylation results, including the observations of enhanced surface expression of ΔF508-CFTR by the ectopic expression of Sar1-T39N, Arf1-Q71L, and STX5. Surface expression of CFTR after blockade of ER-to-Golgi transport was also examined using immunofluorescence microscopy. In control cells with membrane permeabilization (Figure 1F), most of the WT-CFTR is expressed at the cell surface. When conventional ER-to-Golgi trafficking was blocked by Arf1-Q71L, a large amount of WT-CFTR is confined in the ER. However, a significant fraction of WT-CFTR was still found on the plasma membrane. More importantly, a significant amount of ΔF508-CFTR, that was located only in the ER in control cells, reached the cell surface when ER-to-Golgi trafficking was blocked by Arf1-Q71L (Figure 1F). Surface expression of ΔF508-CFTR induced by Arf1-Q71L was more evident in immunostainings using nonpermeabilized cells (Figure 1G).

A key question is whether these immature, core-glycosylated WT and ΔF508 CFTRs unconventionally transported to the cell surface are functional. This was determined by measuring CFTR-mediated $Cl^-$ current in HEK293 cells after ER-to-Golgi blockade (Figures 1H and 1I). Currents generated by CFTR

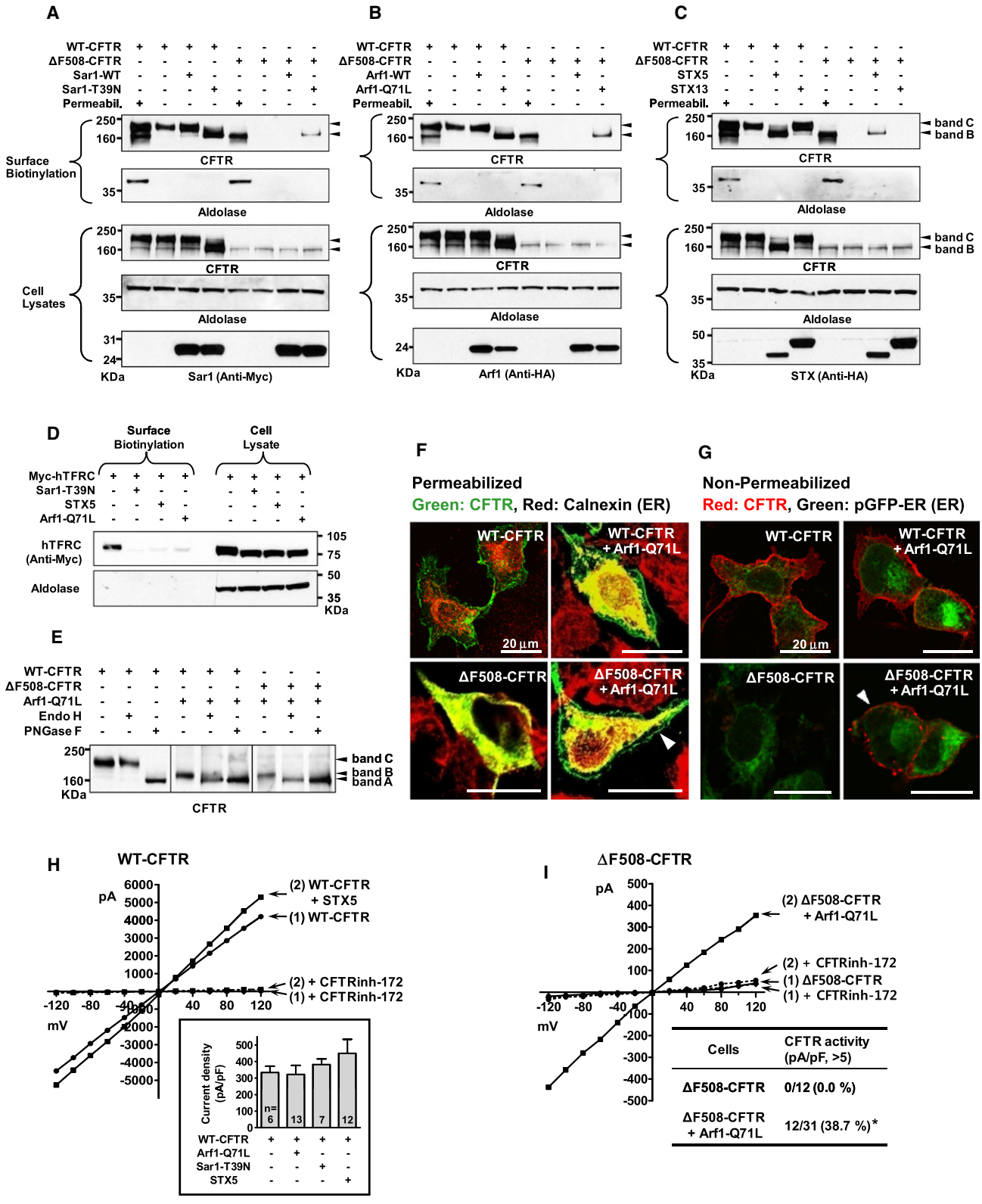


**Figure 1. Surface Expression of Core-Glycosylated CFTR after the Blockade of ER-to-Golgi Traffic in HEK293 Cells**

Bar graph values are mean ± SEM of indicated numbers. band B, immature ER core-glycosylated CFTR; band C, mature complex-glycosylated CFTR; *$p < 0.05$; difference from ΔF508-CFTR alone.

were confirmed by the following three characteristics: (1) activation of $Cl^-$ current by an elevation in cAMP levels (forskolin treatment), (2) a linear I-V relationship, and (3) inhibition of $Cl^-$ current by the CFTR inhibitor CFTRinh-172. As shown in Figure 1H, WT-CFTR $Cl^-$ currents in cells with ER-to-Golgi blockade were comparable to those in control cells. This result indicates that the unconventionally traveled CFTR retains $Cl^-$ channel activity at the cell surface. Most significantly, surface-expressed ΔF508-CFTR due to blockade of ER-to-Golgi trafficking also shows substantial $Cl^-$ current in approximately 40% of cells examined (Figure 1I).

## GRASPs Are Involved in the Unconventional Transport of Core-Glycosylated CFTR to the Plasma Membrane

To characterize the unconventional trafficking route, we examined possible factors involved in the surface transport of core-glycosylated WT and ΔF508-CFTR (Figures 2A and 2B). Incubation at a reduced temperature of 20°C, which blocks trans-Golgi network (TGN)-to-plasma membrane transport (Miller et al., 1992), had no effect on the unconventional transport of core-glycosylated CFTRs, while it blocked the conventional trafficking of complex-glycosylated WT-CFTR (leftmost panel in Figure 2A). However, the surface transport of core-glycosylated CFTRs was blocked by treatments with NEM and nocodazole (second and third panels in Figures 2A and 2B). NEM inhibits membrane fusion by disrupting SNARE functions (Hong, 2005). Although NEM may partially reduce surface expression of CFTR by inhibiting membrane recycling, a complete absence of unconventionally transported core-glycosylated CFTR from the cell surface suggests that NEM-sensitive factors are involved in this process. Nocodazole depolymerizes microtubules. Thus, the pathway by which core-glycosylated CFTR maneuvers to the plasma membrane is NEM-sensitive and microtubule-dependent, but does not appear to involve conventional TGN-to-plasma membrane transport.

A mechanism that can induce exocytosis of the ER protein is the direct fusion of ER membranes to the plasma membrane. STX18, an ER-localized t-SNARE, is known to be involved in ER-mediated phagocytosis, in which direct membrane fusion between the ER and plasma membrane occurs (Hatsuzawa et al., 2006). However, depletion of STX18 by small interfering RNA (siRNA) did not alter the unconventional surface transport of CFTR (Figure S3A). In addition, siRNA- or dominant negative mutation-mediated inhibition of STX3, Rab1, Rab6, and Rab11 that are all known to be involved in the cellular CFTR trafficking (Tang et al., 2011), had no effect on the transport of core-glycosylated CFTR to the cell surface (Figure S3).

Recently, the GRASP homologs in *Dictyostelium* and *Drosophila* were reported to mediate the Golgi-independent unconventional transport of soluble cytosolic and integral membrane proteins (Kinseth et al., 2007; Schotman et al., 2008). Of the two mammalian GRASP isoforms, GRASP55 is expressed in HEK293 cells (Figure 2C). To examine whether GRASP is required for the surface transport of core-glycosylated CFTR, we inhibited endogenous GRASP55 function by treatment with either the dominant-negative GRASP55-G2A mutant or GRASP55-specific siRNA (Figures 2D and 2E). The G2A mutation causes membrane dissociation of GRASP by inhibiting its myristoylation (Shorter et al., 1999). Inhibition of GRASP function by the G2A mutation or by siRNA treatment did not alter the conventional Golgi-mediated trafficking of WT-CFTR (Figure 2D). By contrast, inhibition of GRASP55 abolished the unconventional membrane transport of WT and ΔF508 CFTRs induced by the blockade of ER-to-Golgi trafficking (Figures 2D and 2E). In addition, loss of GRASP function by G2A mutation or siRNA treatment abolished the thapsigargin-induced surface expression of ΔF508-CFTR in CFPAC-1 and HEK293 cells (Figure S4). These findings indicate that GRASPs play a critical role in the surface trafficking of core-glycosylated CFTRs.

## Physical Interaction between GRASP and CFTR

Next, we asked whether CFTR and GRASP interact with each other. Figures 3A and 3B illustrate the domain structures of CFTR and GRASP55 and the constructs made for the protein-protein interaction studies. When coexpressed, GRASP55 does not interact with CFTR in a resting state. Notably, blockade of the conventional exocytic route by Sar1-T39N or STX5 overexpression resulted in an association between core-glycosylated CFTR and GRASP55 (Figure 3C). Sequential truncation from the C terminus indicate that a C-terminal region of CFTR (aa 1386–1480) is responsible for its association with GRASP55 (Figure 3D). Further analyses revealed that deletion of the PDZ (PSD-95/discs large/ZO-1)-binding motif located at the very end of the C terminus, but not deletion of N terminus of CFTR, abolished the

(A–C) Surface biotinylation of CFTR. Blockade of conventional ER-to-Golgi traffic by Sar1-T39N, Arf1-Q71L, and STX5 overexpression induces the cell surface expression of the immature core-glycosylated form (band B) of wild-type (WT) and ΔF508 CFTR. Absence of the cytosolic protein aldolase A in the biotinylated fraction confirms cell surface protein-specific labeling in each experiment. The cells in lanes 1 and 5 were permeabilized with Triton X-100 (0.05%) to show cytosolic CFTR and aldolase A in the surface biotinylation blot as controls. Anti-Myc or anti-HA blot represents the correct expression of each transfected construct.

(D) Surface biotinylation of human transferrin receptor 1 (hTFRC).

(E) Surface biotinylated WT and ΔF508 CFTRs were treated with endoglycosidase H (Endo H) that deglycosylates ER core-glycosylation but not complex-glycosylation, and with N-Glycosidase F (PNGase F) that deglycosylates all N-glycan chains to remove carbohydrate residues from proteins (band A).

(F and G) Immunocytochemistry in membrane permeabilized (F) or nonpermeabilized conditions (G). CFTR was costained with the ER marker protein calnexin or pEYFP-ER. Arrow head indicates surface expression of ΔF508-CFTR after blockade of the conventional ER-to-Golgi traffic by Arf1-Q71L.

(H) Whole-cell $Cl^-$ currents of WT-CFTR. CFTR was activated by the adenylyl cyclase activator forskolin (5 μM) and inhibited by the CFTR inhibitor CFTRinh-172 (10 μM). The current-voltage (I-V) relationships were obtained with a stepwise pulse from −120 mV to +120 mV. Inset: Mean currents at −80 mV were normalized as current densities.

(I) Whole-cell $Cl^-$ currents of ΔF508-CFTR. Inset: Quantal analysis of CFTR channel activity. Current densities greater than five were considered positive CFTR channel activity.

See also Figures S1 and S2.

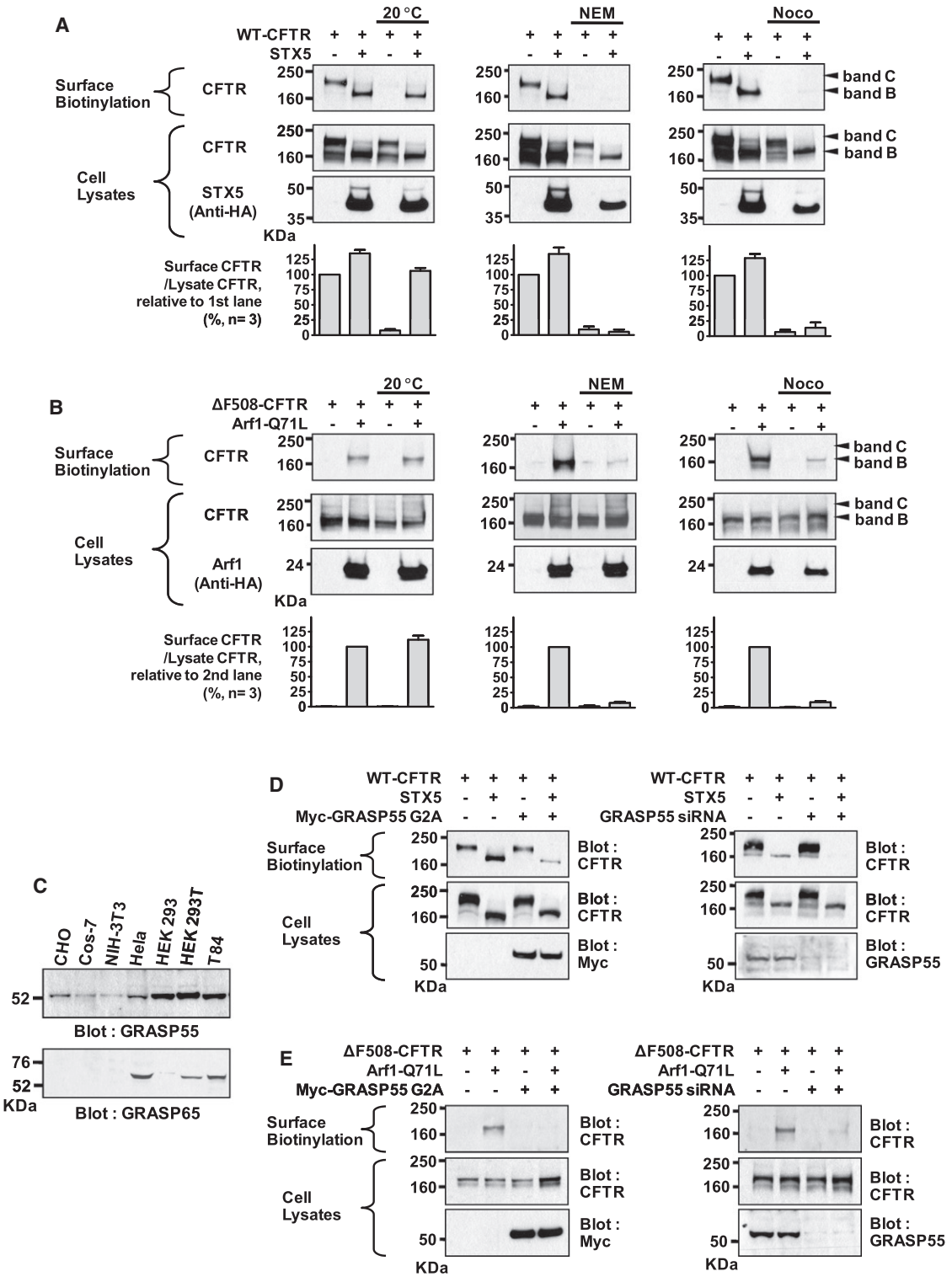


**Figure 2. GRASP Is Involved in the Unconventional Trafficking of Core-Glycosylated CFTR**

(A and B) HEK293 cells were transfected with WT (A) or ΔF508-CFTR (B), and surface biotinylated. STX5 overexpression or Arf1-Q71L was used to block conventional trafficking. Twenty-four hours after transfection, batches of cells were (1) incubated at 20°C for 24 hr, (2) incubated at 20°C for 2 hr then treated with N-ethylmaleimide (NEM; 1 mM) for 15 min and further incubated in serum-free media without NEM for 2 hr at 37°C, or (3) treated with nocodazole (10 μM, 24 hr). Data are shown as mean ± SEM. Other legends are the same as in Figures 1A–1C.

(C) Expression of GRASP55 and GRASP65 in various cell lines.

interaction with GRASP (Figures 3E and 3F). Accordingly, the results of pull-down assays with domain-specific GRASP55 proteins indicate that the first PDZ domain (PDZ1) of GRASP55 binds to the C terminus of CFTR (Figure 3G). Results in Figure 3H show that deletion of the C-terminal PDZ binding motif of CFTR ($\Delta C_4$) abolishes the ER-to-Golgi blockade- and thapsigargin-induced surface expression of ΔF508-CFTR. Collectively, the above results indicate that GRASP directly associates with CFTR via the PDZ domain when ER-to-Golgi transport is blocked, and that this PDZ-mediated interaction is critical for the unconventional surface expression of core-glycosylated CFTR via GRASP.

## ER Stress Signaling Activates the GRASP-Dependent Pathway and Induces Phosphorylation of GRASP

Next, we investigated how the blockade of ER-to-Golgi transport activates the GRASP-dependent unconventional secretory route. Several findings have implicated the involvement of the ER stress response in the activation of this unconventional trafficking. Blockade of the ER-to-Golgi transport including treatment with brefeldin A leads to an accumulation of secretory proteins in the ER lumen and induces UPR (Pahl, 1999). Thapsigargin, which perturbs ER function by depleting ER lumenal calcium stores, is also a well-known agent that induces UPR in mammalian cells (Pahl, 1999). As shown in Figure S4, thapsigargin induced the surface expression of core-glycosylated CFTR via the GRASP-dependent pathway in CFPAC-1 and HEK293 cells. To directly analyze the induction of ER stress signaling, we examined the expression of ER stress marker protein CHOP (C/EBP-homologous protein). Significantly, blockade of the ER-to-Golgi transport by the ectopic expression of STX5, Arf1-Q71L, and Sar1-T39N evoked an induction of CHOP in HEK293 cells (Figure 4A). Three different classes of ER stress signal transducers, IRE1, PERK, and ATF6, have been identified to mediate the UPR (Wiseman et al., 2010). Depletion of each transducer by treatment with specific siRNAs revealed that the IRE1-mediated signaling arm, but not those of PERK and ATF6, is involved in the ER stress-induced exocytosis of core-glycosylated CFTR (Figure 4B).

It has been shown that GRASPs are the substrates of specific signaling cascades, such as the MKK/ERK pathway, and can be phosphorylated during cell division (Jesch et al., 2001). Therefore, we examined whether the ER stress-induced cell signals can affect the phosphorylation status of GRASP. Interestingly, cytosols taken from cells treated with the ER stress-inducing agents (nocodazole and thapsigargin) or cells transfected with the ER-to-Golgi blockade-inducing plasmids evoked an upward shift of recombinant GRASP55, principally the SPR domain of GRASP55, in a band-shift assay (Figure 4C). The control and upward-shifted GRASP55 SPR domains were purified, trypsin-digested, and subjected to a Q-TOF-MS (quadrupole time-of-flight tandem mass spectrometry) analysis to find phosphorylation sites. The tandem mass spectra revealed phosphorylation of the Ser441 residue with a high probability score (Figures 4D–4F).

## GRASP Rescues ΔF508-CFTR in HEK293 Cells in an IRE1- and Ser441 Phosphorylation-Dependent Manner

Next, we investigated whether GRASP upregulation can rescue the defects caused by the ΔF508-CFTR mutation. Notably, overexpression of GRASP55 or GRASP65 alone resulted in surface expression of ΔF508-CFTR in HEK293 cells without significantly inducing ER stress (Figure 5A and Figure S5). In addition, the GRASP-induced, surface-expressed ΔF508-CFTR showed typical CFTR $Cl^-$ currents in whole-cell recording (Figure 5B). As expected, the rescue of ΔF508-CFTR surface expression and $Cl^-$ channel activity by GRASP was abolished by deleting the C-terminal PDZ ligand ($\Delta C_4$) of ΔF508-CFTR (Figures 5C and 5D). These findings further support the notion that a specific interaction with GRASP is important for the rescue of ΔF508-CFTR.

Because IRE1-mediated signaling is required for the thapsigargin-induced surface trafficking of ΔF508-CFTR (Figure 4B), we tested whether the GRASP overexpression-induced trafficking also requires IRE1. As shown in Figure 5E, depletion of IRE1α inhibited the GRASP55 overexpression-induced surface trafficking of ΔF508-CFTR. Furthermore, phosphorylation at the Ser441 residue of GRASP55 was critical for this process. Thus, the phospho-inhibiting mutation of S441A greatly diminished the GRASP55-induced ΔF508-CFTR surface trafficking, while a phospho-mimicking mutation of S441D did not (Figure 5F). These results imply that phosphorylation of GRASP that is associated with the basal activity of IRE1 is critically involved in the GRASP-mediated surface trafficking of ΔF508-CFTR. A recent study has suggested that the unconventional GRASP-mediated secretion of *P. pastoris* Acb1 is dependent on autophagosome formation (Manjithaya et al., 2010). In the case of CFTR, depletion of components involved in the autophagosome formation (ATG1, ATG5, ATG7, and ATG8), but not in lysosome fusion (Vamp7), inhibited unconventional surface trafficking of ΔF508-CFTR induced by thapsigargin or GRASP55 overexpression (Figure S6).

## Transgenic Expression of GRASP Rescues ΔF508-CFTR in Mice

To determine whether GRASP-mediated surface transport of CFTR is indeed of pathophysiological relevance in vivo, we examined the effects of GRASP upregulation on ΔF508-CFTR transport and activity in mice. Transgenic mice harboring GRASP55 (TgGRASP55) were generated and crossed with ΔF508-CFTR mice ($Cftr^{F508\ del}$) mice (Zeiher et al., 1995) (Figures 6A and 6B). Mice homozygous for WT-CFTR or ΔF508-CFTR were used in subsequent experiments. TgGRASP55 mice showed no significant abnormalities in gross appearance up to the age of 1 year. However, $Cftr^{F508\ del}$ mice exhibited marked growth retardation as reported previously (Namkung et al., 2005; Zeiher et al., 1995). Importantly, TgGRASP55 expression completely reversed growth retardation of the $Cftr^{F508\ del}$ mice (Figures 6C and 6D). All $Cftr^{F508\ del}$ mice survived for less than 10 weeks. Most notably, TgGRASP55 expression greatly improved survival of

(D and E) The dominant-negative GRASP55-G2A mutant or GRASP55 depletion by siRNA treatment blocks the unconventional membrane trafficking of WT (D) and ΔF508-CFTR (E). Cells in the right-hand panels were treated with equal amount of control scrambled or GRASP55-specific siRNA (100 nM).
See also Figures S3 and S4.

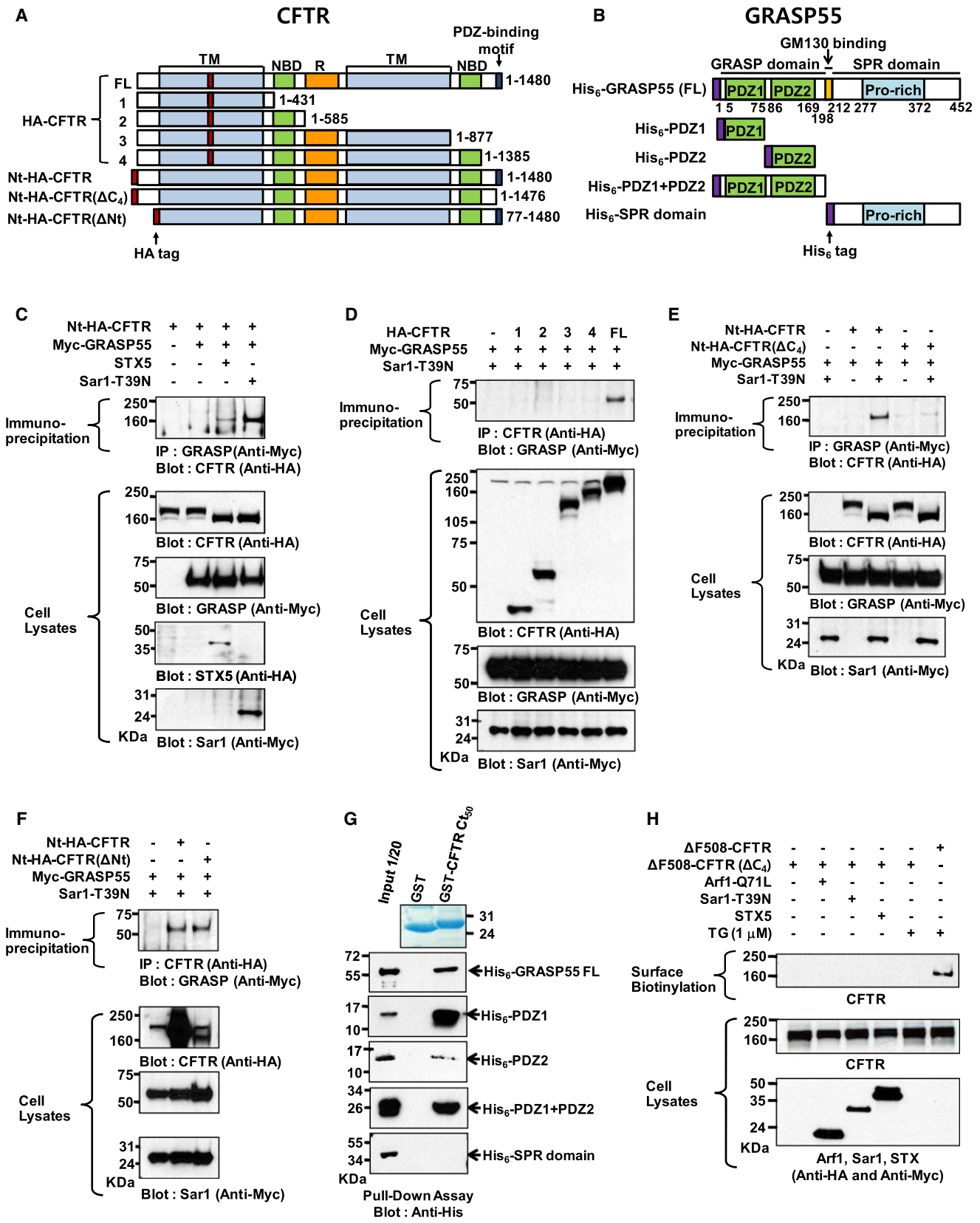
A
CFTR
PDZ-binding motif
TM
NBD
R
TM
NBD
FL
1
2
3
4
HA-CFTR
1-1480
1-431
1-585
1-877
1-1385
Nt-HA-CFTR
Nt-HA-CFTR(ΔC4)
Nt-HA-CFTR(ΔNt)
1-1480
1-1476
77-1480
HA tag
B
GRASP55
GM130 binding
GRASP domain
SPR domain
His6-GRASP55 (FL)
PDZ1
PDZ2
Pro-rich
1 5 75 86 169 198 212 277 372 452
His6-PDZ1
His6-PDZ2
His6-PDZ1+PDZ2
His6-SPR domain
His6 tag
C
Nt-HA-CFTR + + + +
Myc-GRASP55 - + + +
STX5 - - + -
Sar1-T39N - - - +
Immuno-precipitation
250
160
IP : GRASP(Anti-Myc)
Blot : CFTR (Anti-HA)
Cell Lysates
250
160
Blot : CFTR (Anti-HA)
75
50
Blot : GRASP (Anti-Myc)
50
35
Blot : STX5 (Anti-HA)
31
24
KDa
Blot : Sar1 (Anti-Myc)
D
HA-CFTR - 1 2 3 4 FL
Myc-GRASP55 + + + + + +
Sar1-T39N + + + + + +
Immuno-precipitation
75
50
IP : CFTR (Anti-HA)
Blot : GRASP (Anti-Myc)
Cell Lysates
250
160
105
75
50
Blot : CFTR (Anti-HA)
75
50
Blot : GRASP (Anti-Myc)
31
24
KDa
Blot : Sar1 (Anti-Myc)
E
Nt-HA-CFTR - + + - -
Nt-HA-CFTR(ΔC4) - - - + +
Myc-GRASP55 + + + + +
Sar1-T39N + - + - +
Immuno-precipitation
250
160
IP : GRASP (Anti-Myc)
Blot : CFTR (Anti-HA)
Cell Lysates
250
160
Blot : CFTR (Anti-HA)
75
50
Blot : GRASP (Anti-Myc)
31
24
KDa
Blot : Sar1 (Anti-Myc)
F
Nt-HA-CFTR - + -
Nt-HA-CFTR(ΔNt) - - +
Myc-GRASP55 + + +
Sar1-T39N + + +
Immuno-precipitation
75
50
IP : CFTR (Anti-HA)
Blot : GRASP (Anti-Myc)
Cell Lysates
250
160
Blot : CFTR (Anti-HA)
75
50
31
24
KDa
Blot : Sar1 (Anti-Myc)
G
Input 1/20
GST
GST-CFTR Ct50
31
24
72
55
His6-GRASP55 FL
17
10
His6-PDZ1
17
10
His6-PDZ2
34
26
His6-PDZ1+PDZ2
55
34
His6-SPR domain
KDa
Pull-Down Assay
Blot : Anti-His
H
ΔF508-CFTR - - - - - +
ΔF508-CFTR (ΔC4) + + + + + -
Arf1-Q71L - + - - - -
Sar1-T39N - - + - - -
STX5 - - - + - -
TG (1 μM) - - - - + +
Surface Biotinylation
250
160
CFTR
Cell Lysates
250
160
CFTR
50
35
24
KDa
Arf1, Sar1, STX
(Anti-HA and Anti-Myc)

the $Cftr^{F508\ del}$ mice, resulting in only 5% (one out of 19) mortality during the 3 month observation period (Figure 6E). However, TgGRASP55 expression did not improve growth retardation and mouse survival in CFTR null ($Cftr^{-/-}$) mice (Figure S7), suggesting that the effects of TgGRASP are not associated with the background effects of transgene but are specifically related to the rescue of misfolded CFTR.

The ΔF508-CFTR mutation predominantly induces an intestinal pathology rather than respiratory defects in mice (Namkung et al., 2005; Zeiher et al., 1995). A group of mice was therefore sacrificed at the age of 1 month, and intestinal tissues were isolated for a functional assay. As shown in Figures 7A and 7B, CFTR-dependent short circuit current ($I_{sc}$), which is activated by forskolin and inhibited by the $Na^+$-$K^+$-$2Cl^-$ cotransporter inhibitor bumetanide, is critically reduced in the colon of $Cftr^{F508\ del}$ mice. Notably, TgGRASP55 expression results in resumption of CFTR-dependent $I_{sc}$ in the $Cftr^{F508\ del}$ mouse colon, to 63% of the level in WT mice. Immunohistochemical analyses further indicate that transgenic GRASP expression rescues ΔF508-CFTR in mice (Figure 7C). In wild-type mice, CFTR is expressed at the apical membrane of colonic crypt cells and TgGRASP55 expression does not affect this pattern. The apical expression of CFTR at colonic crypts was not observed in $Cftr^{F508\ del}$ mice as reported earlier (Namkung et al., 2005; Zeiher et al., 1995). Clearly, TgGRASP55 expression rescued the apical expression of ΔF508-CFTR in crypt cells (Figure 7C). Finally, surface biotinylation analyses with samples from mouse colonic mucosa reveal that TgGRASP55 expression induces the surface expression of core-glycosylated ΔF508-CFTR, but not complex-glycosylated CFTR (Figure 7D). These results, taken together, indicate that upregulation of GRASP55 expression in vivo could effectively rescue the CF phenotype resulting from ΔF508-CFTR mutation.

## DISCUSSION

In the present study, we discovered that immature core-glycosylated CFTR can travel to the plasma membrane via the GRASP-dependent unconventional route, and made use of this finding to markedly improve the surface expression of ΔF508-CFTR and to rescue the defects caused by the ΔF508-CFTR mutation in vitro and in vivo. Several unique observations lead to these conclusions. One of these is the surface expression of core-glycosylated WT and ΔF508 CFTRs after ER-to-Golgi blockade. This was shown by multiple assays, including surface biotinylation, surface ELISA, and immunohistochemistry. Moreover, the appearance of $Cl^-$ channel activity typical of CFTR in cells with ER-to-Golgi blockade solidified presence of the Golgi-independent membrane trafficking of WT and ΔF508 CFTRs (Figure 1).

GRASP65 and GRASP55 are two mammalian myristoylated proteins initially shown to be involved in Golgi assembly (Barr et al., 1997; Shorter et al., 1999). However, GrpA, the single homolog of GRASP in *D. discoideum*, has been identified to mediate the unconventional secretion of a soluble cytoplasmic protein AcbA via a Golgi-independent route (Kinseth et al., 2007). Similarly, *D. melanogaster* dGRASP is required for the Golgi-independent membrane trafficking of integral plasma membrane proteins (Schotman et al., 2008). The present study extends these findings to show that mammalian GRASPs are involved in the unconventional Golgi-independent membrane trafficking using CFTR as a model.

An interesting question addressed here is how the blockade of ER-to-Golgi traffic activates the GRASP-dependent unconventional exocytosis. Several findings in the present study indicate that ER stress signals are involved in this unconventional trafficking. Transit from the ER to the Golgi complex is the rate-limiting step in the secretion of many glycoproteins (Schröder and Kaufman, 2005). Blockade of the conventional ER-to-Golgi transport evoked an induction of the UPR marker protein CHOP in HEK293 cells (Figure 4A). The well-known UPR-inducing agents, thapsigargin and brefeldin A, induced GRASP-dependent surface expression of core-glycosylated CFTR (Figures S1 and S4). Moreover, depletion of IRE1α abolished this unconventional exocytosis (Figures 4B and 5E). In general, UPR decreases the ER folding demand by inhibiting transcription and translation of secretory proteins and by increasing clearance of unfolded proteins through ERAD. UPR also increases the folding capacity of the ER by promoting synthesis of ER-resident chaperones and by increasing the size of the ER (Ron and Walter, 2007; Schröder and Kaufman, 2005). In addition to these well-known functions, the present results suggest that ER stress may activate the secretion of ER proteins via the unconventional route to relieve the protein burden. Further investigations with other forms of ER stress, such as increased ER flux or treatments with tunicamycin and dithiothreitol, will reveal the general importance of unconventional trafficking in ER stress responses.

Upregulation of GRASP function alone resulted in surface expression of ΔF508-CFTR without inducing the proapototic CHOP signals in HEK293 cells (Figure 5 and Figure S5) and rescued defects caused by ΔF508-CFTR without any apparent toxicity in mice (Figures 6 and 7). Although the GRASP overexpression-mediated pathway does not induce the CHOP signals, it requires phosphorylation of the Ser441 residue that is associated with the basal activity of IRE1 (Figures 5E and 5F).

**Figure 3. Protein-Protein Interactions between CFTR and GRASPs**

(A and B) Schematic diagram of CFTR and GRASP constructs used in immunoprecipitation and pull-down assays. FL, full-length; NBD, nucleotide-binding domain; TM, transmembrane domain; R, regulatory domain; SPR, serine/proline-rich.

(C) Protein samples were immunoprecipitated with anti-Myc (GRASP55) and immunoblotted with anti-HA (CFTR). For immunoblotting of cell lysates, 50 μg of proteins were loaded into each lane, and immunoprecipitation was performed with a total of 500 μg of cell lysate.

(D–F) Identification of CFTR domain that interacts with GRASP by using immunoprecipitation. Deletion of the C-terminal PDZ binding motif of CFTR (D and E), but not the deletion of N terminus (F), abolishes its interaction with GRASP55.

(G) Pull-down assays. Expression of glutathione-S-transferase (GST) and the GST-fused CFTR C-terminal 50 amino acids ($Ct_{50}$) was visualized by Ponceau S staining (uppermost panel). GST-pull-down assays were performed using 10 μg of purified recombinant $His_6$-tagged GRASP55 domain and 20 μg of GST-fusion proteins. One microgram of each $His_6$-tagged protein was loaded as an input control. PDZ1 of GRASP55 shows the strongest interaction with CFTR.

(H) Deletion of C-terminal PDZ binding motif ($\Delta C_4$) abolishes cell surface expression of ΔF508-CFTR induced by ER-to-Golgi blockade or thapsigargin (TG).

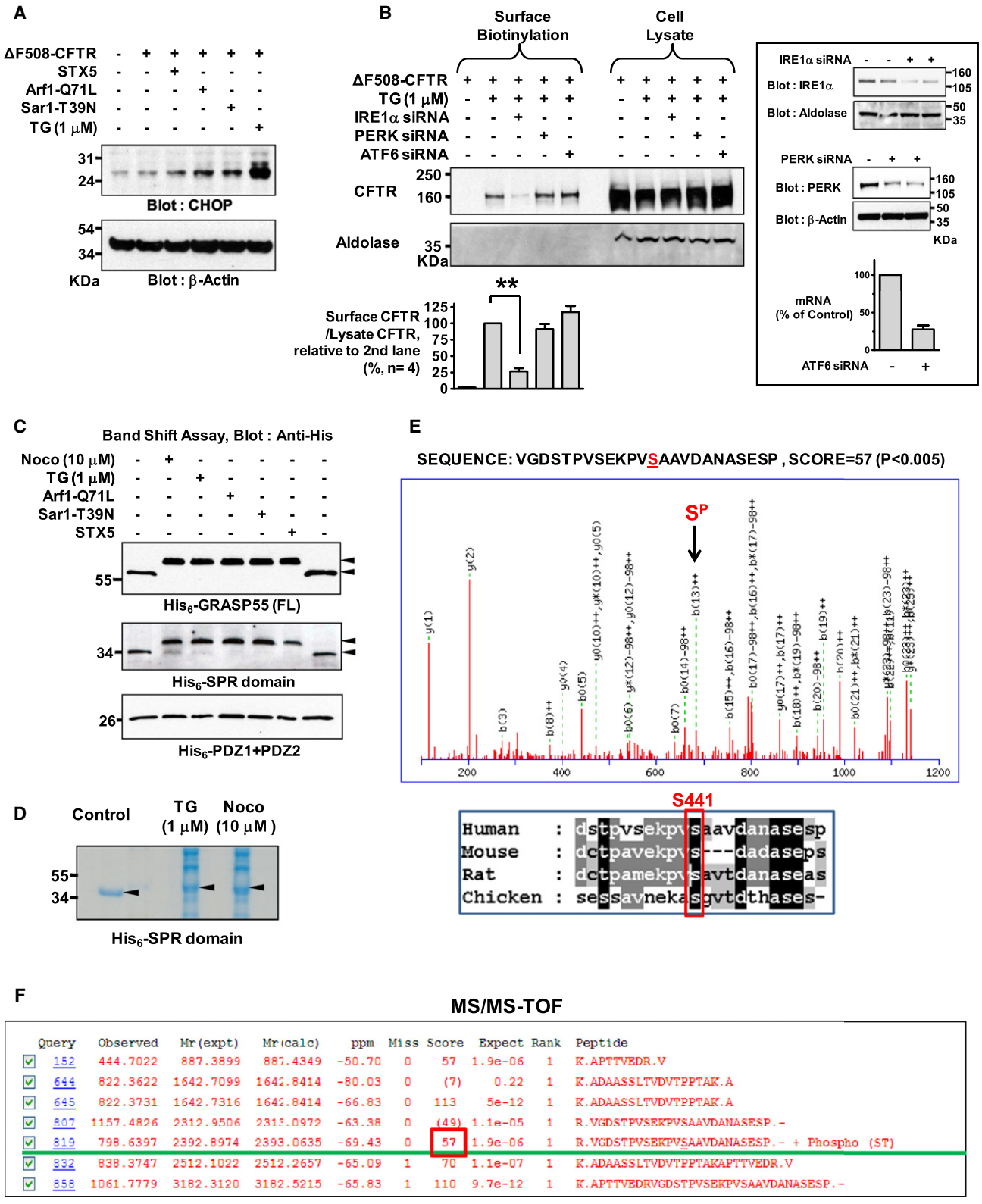


| | Query | Observed | Mr(expt) | Mr(calc) | ppm | Miss | Score | Expect | Rank | Peptide |
|---|---|---|---|---|---|---|---|---|---|---|
| ☑ | 152 | 444.7022 | 887.3899 | 887.4349 | -50.70 | 0 | 57 | 1.9e-06 | 1 | K.APTTVEDR.V |
| ☑ | 644 | 822.3622 | 1642.7099 | 1642.8414 | -80.03 | 0 | (7) | 0.22 | 1 | K.ADAASSLTVDVTPPTAK.A |
| ☑ | 645 | 822.3731 | 1642.7316 | 1642.8414 | -66.83 | 0 | 113 | 5e-12 | 1 | K.ADAASSLTVDVTPPTAK.A |
| ☑ | 807 | 1157.4826 | 2312.9506 | 2313.0972 | -63.38 | 0 | (49) | 1.1e-05 | 1 | R.VGDSTPVSEKPVSAAVDANASESP.- |
| ☑ | 819 | 798.6397 | 2392.8974 | 2393.0635 | -69.43 | 0 | 57 | 1.9e-06 | 1 | R.VGDSTPVSEKPVSAAVDANASESP.- + Phospho (ST) |
| ☑ | 832 | 838.3747 | 2512.1022 | 2512.2657 | -65.09 | 1 | 70 | 1.1e-07 | 1 | K.ADAASSLTVDVTPPTAKAPTTVEDR.V |
| ☑ | 858 | 1061.7779 | 3182.3120 | 3182.5215 | -65.83 | 1 | 110 | 9.7e-12 | 1 | K.APTTVEDRVGDSTPVSEKPVSAAVDANASESP.- |

**Figure 4. Activation of the Unconventional Trafficking of ΔF508-CFTR and Phosphorylation of GRASP by ER Stress Signals**

(A) Induction of the ER stress marker protein CHOP (C/EBP-homologous protein) by the ER-to-Golgi blockade. HEK293 cells were harvested 18 hr after transfection with indicated plasmids or after treatment with thapsigargin (TG) as described in Figure 1S. β-actin blot was used as a loading control.

A well-known function of IRE1 is the activation of the X-box binding protein-1 (XBP1) transcription factor by its endonuclease activity. However, metazoan IRE1 has signaling functions beyond its nucleolytic activity. For example, mammalian IRE1 interacts with tumor necrosis associated factor 2 (TRAF2) and activates the stress-induced Jun N-terminal kinase (JNK) (Urano et al., 2000). Identification of the specific upstream kinase that phosphorylates the Ser441 residue of GRASP55 would be a critical task to selectively modulate the GRASP-dependent unconventional exocytosis. Interestingly, mammals have two IRE1 isoforms, IRE1α and IRE1β. Although the two isoforms appear to have the same in vitro activities and subcellular localizations, gene deletion studies in mice revealed that only IRE1α is essential for mammalian development (Bernales et al., 2006b; Zhang et al., 2005). Whereas IRE1α is expressed in all mammalian cells, IRE1β is expressed primarily in epithelial cells (Bernales et al., 2006b). Therefore, it is tempting to speculate that activation of IRE1β may selectively induce the GRASP-mediated surface trafficking of ΔF508-CFTR in epithelial cells.

Recent reports suggest that UPR activates autophagy pathways (Bernales et al., 2006a). In the present study, factors involved in early autophagosome formation, but not those involved in the late steps of lysosome fusion and degradation pathway, appear to be associated with GRASP-mediated unconventional exocytosis of CFTR in mammalian cells (Figure S6), similar to the unconventional Acb1 secretion in yeast (Manjithaya et al., 2010). However, whether CFTR and Acb1 are transported by the same autophagy-dependent unconventional secretory mechanism is unclear at the moment and remains to be further investigated. Classical autophagy has been characterized primarily as a degradative pathway of macromolecules and their recycling. A growing body of evidence suggests that autophagy pathways have other important cellular functions, ranging from antigen presentation to unconventional protein secretion (Manjithaya and Subramani, 2011). The present results imply that the inhibition of normal conventional secretion under stressed conditions might activate unconventional secretion that selectively utilizes autophagosomal components in mammalian cells. Previously, it was suggested that CFTR can be unconventionally transported from the ER to TGN via an STX5- and Arf1-independent pathway in BHK and CHO cells (Yoo et al., 2002). However, the unconventional ER-to-TGN pathway in BHK cells seems to be different from the GRASP-mediated pathway described here in several aspects. For example, the unconventional ER-to-TGN transport in BHK cells is dependent on Sar1, and eventually complex-glycosylated CFTR is expressed on the cell surface, while the unconventional pathway described in the present study is insensitive to the dominant-negative Sar1 and transports core-glycosylated CFTR to the cell surface. Nonetheless, the collective results indicate that the classical secretory pathway traveling through the ER, all sub-compartments of the Golgi, and secretory vesicles is not the only route for cell surface trafficking of CFTR.

Another notable and important finding of this study is the directional transport of ΔF508-CFTR to the apical membrane of colonic crypt cells in TgGRASP55 mice (Figure 7C). It has been shown that dGRASP mediates the Golgi-independent transport of integrin α subunit to a specific basolateral membrane area, called the zone of contact, at specific developmental stages in *Drosophila* (Schotman et al., 2008). Therefore, it seems that the unconventional pathway mediated by GRASPs recognizes specific sorting determinant of its cargo molecules and facilitates their transport to the destined location in the plasma membrane. Domain-specific interaction of GRASP and CFTR (Figure 3) also supports the concept of cargo-specificity in the GRASP-mediated tethering of cargo molecules.

We propose that GRASPs are one of the tethering factors that (1) are involved in the ER stress-induced unconventional secretion, (2) specifically associate with cargo molecules through their PDZ domains, and (3) are activated by specific upstream kinases. Future studies investigating the specific upstream signals and downstream trafficking machinery should identify pharmacologically suitable therapeutic targets to treat diseases stemming from misfolded proteins with trafficking defects. Although general upregulation of GRASP function by transgenic gene expression sufficiently corrects the defects caused by the ΔF508-CFTR mutation in mice, specific activation of native GRASP or related proteins should be considered as an important therapeutic approach. Small molecules that can reproduce the effect of GRASP overexpression will be highly desirable and applicable for the treatment of human patients with CF.

## EXPERIMENTAL PROCEDURES

For a detailed description of all the methods, please see the Extended Experimental Procedures and Table S1.

### Cell Culture, Plasmids, siRNA, and Antibodies

HEK293 and CFPAC-1 cells were maintained in culture media supplemented with serum and antibiotics. Information for plasmids, siRNAs, and antibodies used in this study is available in the relevant sections of the Extended Experimental Procedures.

(B) The ER stress-induced unconventional trafficking of ΔF508-CFTR is blocked by the knockdown of IRE1α. Surface biotinylation was performed after transfection with control scrambled siRNA or siRNAs specific for IRE1α, PERK, and ATF6 (50 nM each). Inset: A 75%–90% loss of each UPR transducer protein was confirmed by relevant immunoblotting or real-time PCR. Data are shown as mean ± SEM.

(C) Detection of GRASP55 phosphorylation using a band-shift assay. Recombinant full-length (FL) or domain-specific GRASP55 proteins (200 ng; see Figures 3B and 3G) were incubated with cytosol taken from HEK293 cells (500 μl, for 60 min at 37°C) and immunoblotted with anti-His antibodies. HEK293 cells were treated with DMSO (0.1%, solvent control), nocodazole (Noco), or thapsigargin (TG), or transfected with each plasmid as described previously. Arrowheads indicate an upward shift of protein bands.

(D–F) Identification of the ER stress signal-induced phosphorylation site of GRASP55 using the quadrupole time-of-flight tandem mass spectrometer (Q-TOF-MS) analysis. Purified GRASP55 SPR domains (10 μg) were separated by SDS-PAGE and visualized via Coomasie blue staining (D). Then, the protein bands were excised from gels, trypsin-digested, and analyzed with Q-TOF to find phosphorylation sites. Product ion spectra obtained from samples of the TG-cytosol detected a phospho peptide (S, phosphoserine). The phosphorylation site corresponds to the Ser441 residue of human GRASP55, which is highly conserved among vertebrate GRASP55s. (E) and (F) represent tandem mass spectra and query results of the Mascot database, respectively.

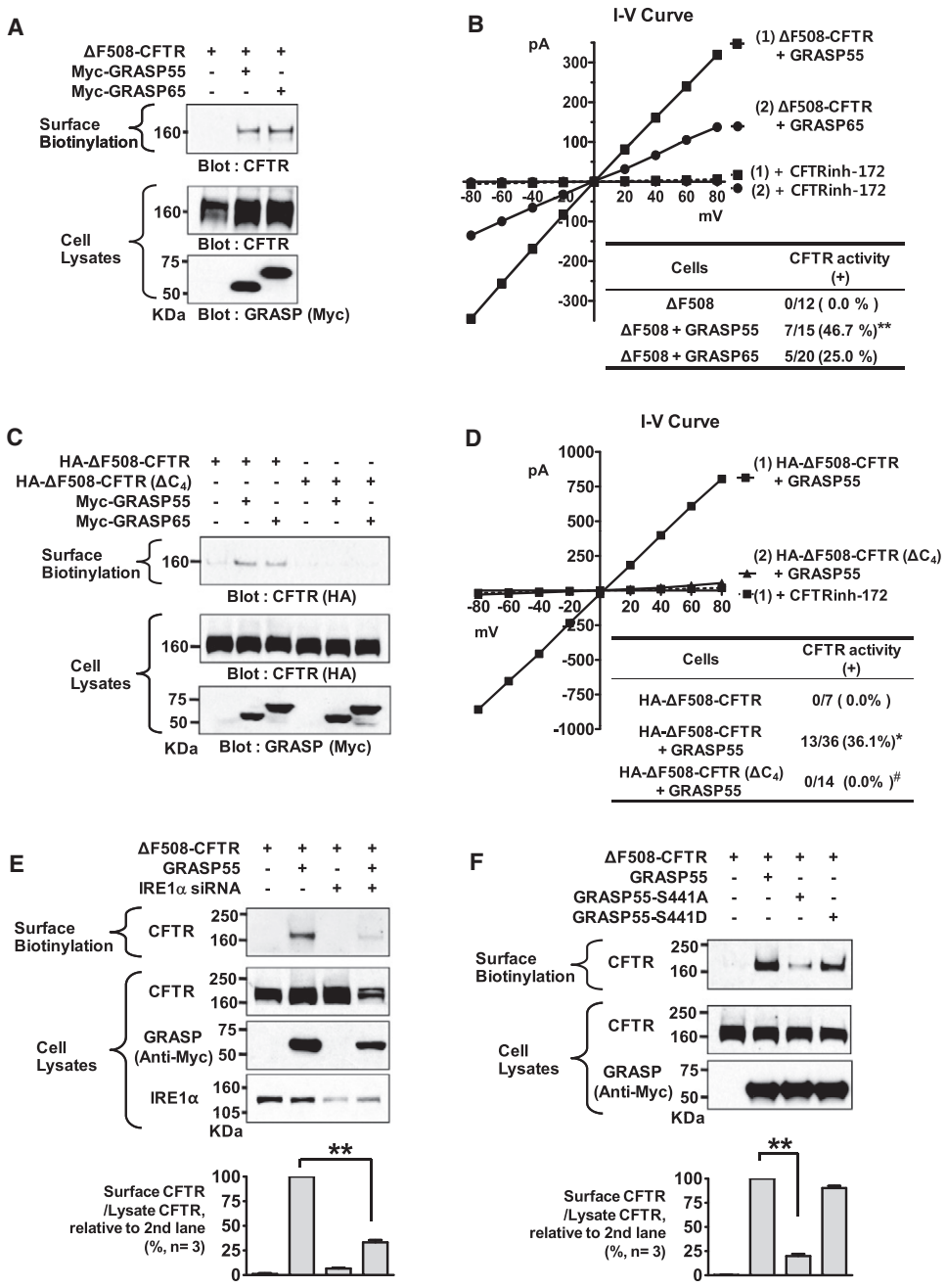


**Figure 5. Rescue of ΔF508-CFTR by the Upregulation of GRASP in HEK293 Cells**

Bar graph values are mean ± SEM.

(A and B) Heterologous expression of GRASP55 or GRASP65 induces the cell surface expression of ΔF508-CFTR and apparent CFTR $Cl^-$ channel activities. Insets in (B) and (D) represent quantal analysis of CFTR channel activity. Current densities greater than five were considered positive CFTR channel activity. **$p < 0.01$; difference from ΔF508-CFTR alone.

(C and D) The GRASP-induced surface expression of ΔF508-CFTR (C) and its $Cl^-$ channel activities (D) were abolished when the C-terminal PDZ binding motif of ΔF508-CFTR was deleted ($\Delta C_4$). *$p < 0.05$; difference from ΔF508-CFTR alone, $^{\#}p < 0.05$; difference from HA-ΔF508-CFTR + GRASP55.

(E) IRE1α is required for the GRASP55-mediated surface trafficking of ΔF508-CFTR. Surface expression of CFTR was examined after transfection with indicated plasmids and the control scrambled or IRE1α siRNA (50 nM each). **$p < 0.01$.

(F) The phospho-inhibiting mutation of S441A inhibits the GRASP55-induced surface trafficking of ΔF508-CFTR, while the phospho-mimicking mutation of S441D does not. **$p < 0.01$.

See also Figures S5 and S6.

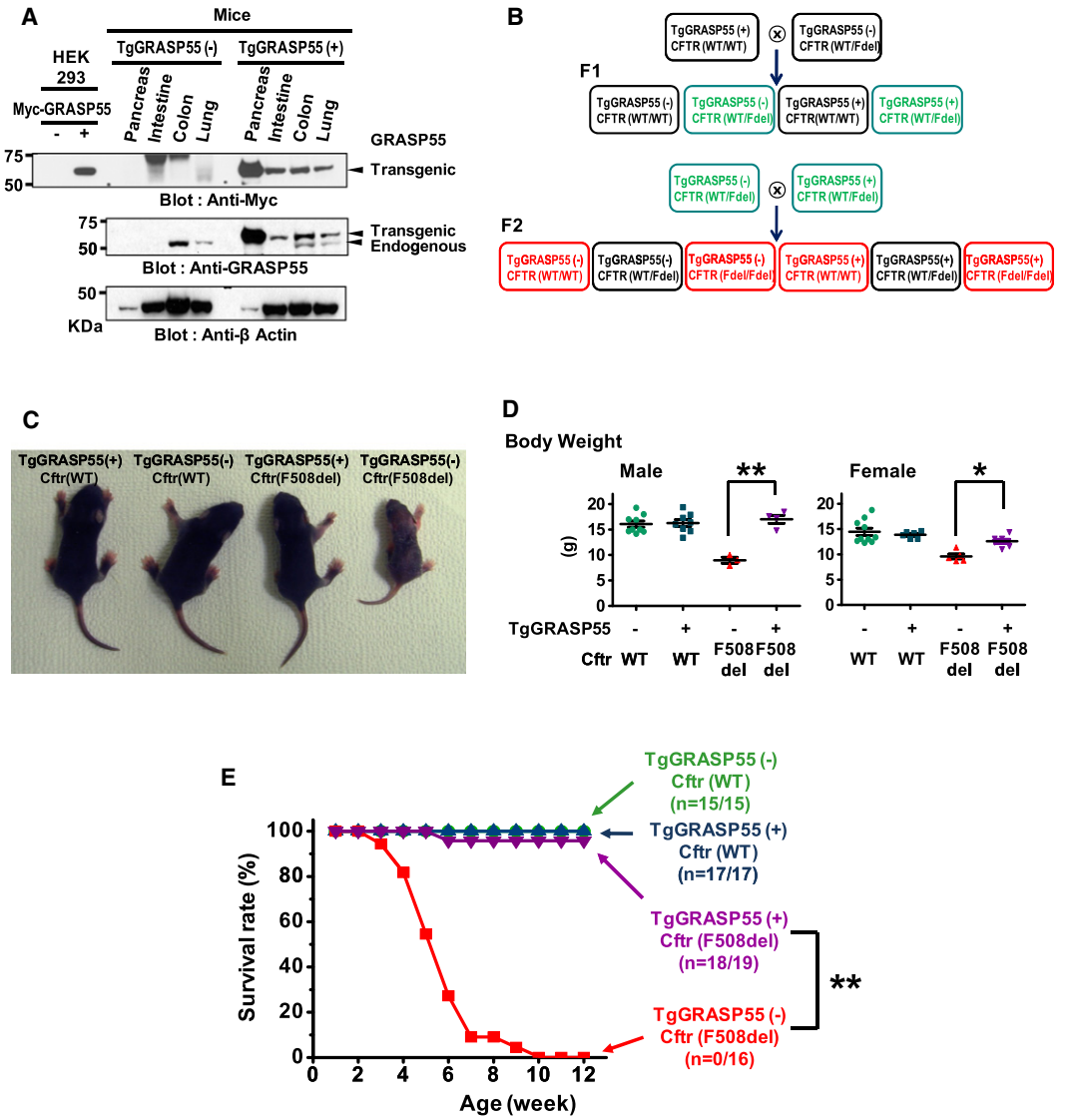


**Figure 6. Transgenic GRASP Expression Rescues Mouse Survival in Cftr$^{F508\ del}$ Mice**

(A) Characterization of transgenic mice harboring GRASP55 (TgGRASP55). Immunoblot of various tissue lysates (60 μg) from GRASP55-negative and GRASP55-positive littermates of TgGRASP55 mice. TgGRASP55-positive mice express transgenic Myc-hGRASP55, and its expression is an average of 3.7-fold higher than that of endogenous GRASP55 in the colon. Lysates from HEK293 cells (10 μg) were used as a positive control for Myc-GRASP55.

(B) TgGRASP55(+) mice were crossed with heterozygous Cftr$^{F508\ del}$ mice, and four groups of mice homozygous for either WT-CFTR or ΔF508-CFTR in the F2 generation (red rectangle) were used in this study.

(C and D) Mouse growth. Mouse picture was taken at the age of 10 days (C), and body weight was quantified at the age of 30 days (D). Cftr$^{F508\ del}$ mice show significant growth retardation, and TgGRASP55 expression restores weight gain. Data are shown as mean ± SEM. *$p < 0.05$, **$p < 0.01$.

(E) Survival analyses. TgGRASP55 expression greatly improves the survival of Cftr$^{F508\ del}$ mice, resulting in 95% (18 out of 19) survival at the age of 12 weeks, compared to 0% survival in control Cftr$^{F508\ del}$ mice. **$p < 0.01$.

See also Figure S7.

### Mice

Cftr$^{F508\ del}$ mice were obtained from K.R. Thomas (University of Utah, Salt Lake City, UT) (Zeiher et al., 1995) and Cftr$^{-/-}$ (B6.129P2-Cftr$^{tm1Unc}$/J) mice were purchased from the Jackson Laboratory. TgGRASP55 mice were generated in this study. Cftr$^{WT/F508\ del}$ and Cftr$^{+/-}$ mice were crossed with TgGRASP55(+) mice to express TgGRASP55 in mice homozygous for Cftr$^{F508\ del/F508\ del}$ or Cftr$^{-/-}$.

### Immunoblotting, Immunoprecipitation, Pull-Down Assay, and Immunofluorescence Staining

Immunoblotting and immunoprecipitation were performed as described previously (Gee et al., 2009). The pull-down assay was performed as described previously (Lee et al., 2007). Immunofluorescence staining of mouse colons was performed with anti-CFTR R4 rabbit polyclonal antibody as described previously (Gee et al., 2010).

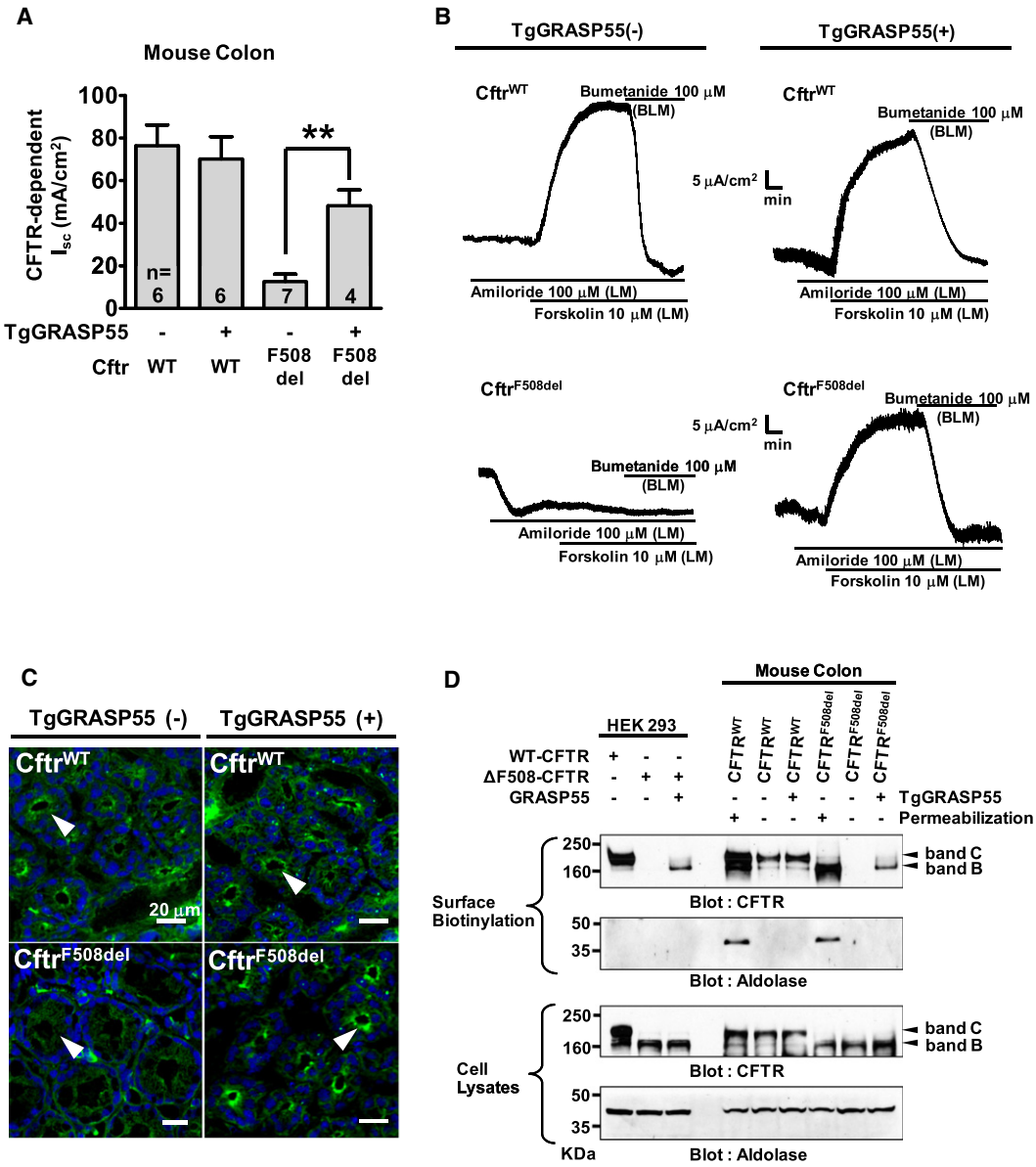


**Figure 7. Transgenic GRASP Expression Rescues Surface Expression of ΔF508-CFTR and $I_{sc}$ in the Colon of $Cftr^{F508\ del}$ Mice**

(A and B) Short circuit current ($I_{sc}$) measurements in the mouse colon. Mice homozygous for WT-CFTR or ΔF508-CFTR at the age of 1 month were sacrificed and $I_{sc}$ was measured. Forskolin (10 μM) application to the apical side evoked a lumen-negative $I_{sc}$ that is fully inhibited by basolateral application of the $Na^+$-$K^+$-$2Cl^-$ cotransporter inhibitor bumetanide (100 μM). The apical side was treated with amiloride (100 μM) to block epithelial $Na^+$ channels. TgGRASP55 expression results in the apparent CFTR-dependent $I_{sc}$ in the $Cftr^{F508\ del}$ mouse colon. A summary of multiple experiments and representative traces of $I_{sc}$ measurements are presented in panels (A) and (B), respectively. Values are mean ± SEM of indicated numbers. **$p < 0.01$.

(C) Immunostaining. Cross-sections of mouse colonic crypts were immunostained with anti-CFTR R4 rabbit polyclonal antibody. TgGRASP55 expression results in the rescue of CFTR expression at the apical membrane of crypt cells in the $Cftr^{F508\ del}$ mouse colon. Arrowheads indicate the apical region of colonic crypts.

(D) Epithelial cells were harvested from colonic mucosa, and surface biotinylation was performed. Some cells were permeabilized with Triton X-100 (0.05%) to show cytosolic CFTR and aldolase A in the surface biotinylation blot. Note that TgGRASP55 expression in mouse colon induces the cell surface expression of immature core-glycosylated ΔF508-CFTR (band B).

### Surface Biotinylation and Surface ELISA

Surface biotinylation of CFTR was performed as described previously (Han et al., 2006). Surface ELISA was performed using the extracellular HA epitope-tagged CFTR construct as described previously (Gee et al., 2010).

### Real-Time and Reverse-Transcription PCR Analysis

RNA samples were subjected to the reverse-transcription (RT)-PCR reaction with an AccuScript High Fidelity 1st Strand cDNA Synthesis Kit (Stratagene, La Jolla, CA) according to the manufacturer's instructions. Real-time RT-PCR analyses were executed for evaluating efficiency of siRNAs.

### Band-Shift Assay and Q-TOF-MS Analysis

For detection of GRASP55 phosphorylation, a band-shift assay and subsequent Q-TOF-MS analysis were performed. Detailed procedures are given in the Extended Experimental Procedures.

### Measurements of $Cl^-$ Channel Activity and Shot-Circuit Current

Whole-cell recordings were performed on HEK293 cells as reported previously (Namkung et al., 2005). For short-circuit current measurements, colon tissue was stripped of connective tissue and muscle, opened longitudinally, and mounted in an Ussing chamber (World Precision Instruments, Stevenage, UK). Tissues were voltage-clamped at 0 mV with an EVC-4000 voltage clamp (World Precision Instruments), and short-circuit currents ($I_{sc}$) were continuously recorded with a PowerLab data acquisition system (AD Instruments, Castle Hill, Australia).

### Statistical and Survival Analyses

Results are presented as mean ± SEM for the indicated number of experiments. Statistical analysis of continuous data was performed with Student's t test or with analysis of variance followed by Tukey's multiple comparison test, as appropriate. Pearson's chi-square test was applied to analyze the quantal data of $Cl^-$ currents in cells expressing ΔF508-CFTR. Survival analysis was performed with the Kaplan-Meier method and differences between the groups were analyzed by the log-rank method. $p < 0.05$ was considered statistically significant.

## SUPPLEMENTAL INFORMATION

Supplemental Information includes Extended Experimental Procedures, seven figures, and one table and can be found with this article online at doi:10.1016/j.cell.2011.07.021.

## ACKNOWLEDGMENTS

We thank Shmuel Muallem, Hyun Woo Park, and Dong-Su Jang for helpful discussions and editorial assistance, and the Yonsei-Carl Zeiss Advanced Imaging Center, Yonsei Proteome Research Center, and the Mouse Division of Macrogen for technical assistance. This work was supported by grants 2011-0001178 and 2011-0016484 from the National Research Foundation of Korea funded by the Ministry of Education, Science, and Technology, Korea, and A030001 from the Korea Health 21 R&D Project, Ministry of Health and Welfare, Korea. B.L.T. is supported by an AcRF grant from the Ministry of Education of Singapore. H.Y.G. and S.H.N. performed the experiments, analyzed data, and wrote the paper. B.L.T. and K.H.K. assisted in performing experiments. M.G.L. designed and coordinated the study and wrote the paper.

Received: January 21, 2011
Revised: June 4, 2011
Accepted: July 8, 2011
Published: September 1, 2011

## REFERENCES

Amaral, M.D. (2004). CFTR and chaperones: processing and degradation. J. Mol. Neurosci. *23*, 41–48.

Barr, F.A., Puype, M., Vandekerckhove, J., and Warren, G. (1997). GRASP65, a protein involved in the stacking of Golgi cisternae. Cell *91*, 253–262.

Becq, F. (2010). Cystic fibrosis transmembrane conductance regulator modulators for personalized drug treatment of cystic fibrosis: progress to date. Drugs *70*, 241–259.

Bernales, S., McDonald, K.L., and Walter, P. (2006a). Autophagy counterbalances endoplasmic reticulum expansion during the unfolded protein response. PLoS Biol. *4*, e423.

Bernales, S., Papa, F.R., and Walter, P. (2006b). Intracellular signaling by the unfolded protein response. Annu. Rev. Cell Dev. Biol. *22*, 487–508.

Denning, G.M., Anderson, M.P., Amara, J.F., Marshall, J., Smith, A.E., and Welsh, M.J. (1992). Processing of mutant cystic fibrosis transmembrane conductance regulator is temperature-sensitive. Nature *358*, 761–764.

Egan, M.E., Glöckner-Pagel, J., Ambrose, C., Cahill, P.A., Pappoe, L., Balamuth, N., Cho, E., Canny, S., Wagner, C.A., Geibel, J., and Caplan, M.J. (2002). Calcium-pump inhibitors induce functional surface expression of Delta F508-CFTR protein in cystic fibrosis epithelial cells. Nat. Med. *8*, 485–492.

Gee, H.Y., Kim, Y.W., Jo, M.J., Namkung, W., Kim, J.Y., Park, H.W., Kim, K.S., Kim, H., Baba, A., Yang, J., et al. (2009). Synaptic scaffolding molecule binds to and regulates vasoactive intestinal polypeptide type-1 receptor in epithelial cells. Gastroenterology *137*, 607–617, 617, e1–e4.

Gee, H.Y., Tang, B.L., Kim, K.H., and Lee, M.G. (2010). Syntaxin 16 binds to cystic fibrosis transmembrane conductance regulator and regulates its membrane trafficking in epithelial cells. J. Biol. Chem. *285*, 35519–35527.

Han, W., Kim, K.H., Jo, M.J., Lee, J.H., Yang, J., Doctor, R.B., Moe, O.W., Lee, J., Kim, E., and Lee, M.G. (2006). Shank2 associates with and regulates $Na^+/H^+$ exchanger 3. J. Biol. Chem. *281*, 1461–1469.

Hatsuzawa, K., Tamura, T., Hashimoto, H., Hashimoto, H., Yokoya, S., Miura, M., Nagaya, H., and Wada, I. (2006). Involvement of syntaxin 18, an endoplasmic reticulum (ER)-localized SNARE protein, in ER-mediated phagocytosis. Mol. Biol. Cell *17*, 3964–3977.

Helms, J.B., and Rothman, J.E. (1992). Inhibition by brefeldin A of a Golgi membrane enzyme that catalyses exchange of guanine nucleotide bound to ARF. Nature *360*, 352–354.

Hong, W. (2005). SNAREs and traffic. Biochim. Biophys. Acta *1744*, 493–517.

Jesch, S.A., Lewis, T.S., Ahn, N.G., and Linstedt, A.D. (2001). Mitotic phosphorylation of Golgi reassembly stacking protein 55 by mitogen-activated protein kinase ERK2. Mol. Biol. Cell *12*, 1811–1817.

Kinseth, M.A., Anjard, C., Fuller, D., Guizzunti, G., Loomis, W.F., and Malhotra, V. (2007). The Golgi-associated protein GRASP is required for unconventional protein secretion during development. Cell *130*, 524–534.

Kunzelmann, K. (2001). CFTR: interacting with everything? News Physiol. Sci. *16*, 167–170.

Lee, J.H., Richter, W., Namkung, W., Kim, K.H., Kim, E., Conti, M., and Lee, M.G. (2007). Dynamic regulation of cystic fibrosis transmembrane conductance regulator by competitive interactions of molecular adaptors. J. Biol. Chem. *282*, 10414–10422.

Luo, Y., McDonald, K., and Hanrahan, J.W. (2009). Trafficking of immature DeltaF508-CFTR to the plasma membrane and its detection by biotinylation. Biochem. J. *419*, 211–219, 2, 219.

Manjithaya, R., and Subramani, S. (2011). Autophagy: a broad role in unconventional protein secretion? Trends Cell Biol. *21*, 67–73.

Manjithaya, R., Anjard, C., Loomis, W.F., and Subramani, S. (2010). Unconventional secretion of Pichia pastoris Acb1 is dependent on GRASP protein, peroxisomal functions, and autophagosome formation. J. Cell Biol. *188*, 537–546.

Miller, S.G., Carnell, L., and Moore, H.H. (1992). Post-Golgi membrane traffic: brefeldin A inhibits export from distal Golgi compartments to the cell surface but not recycling. J. Cell Biol. *118*, 267–283.

Namkung, W., Kim, K.H., and Lee, M.G. (2005). Base treatment corrects defects due to misfolding of mutant cystic fibrosis transmembrane conductance regulator. Gastroenterology *129*, 1979–1990.

Pahl, H.L. (1999). Signal transduction from the endoplasmic reticulum to the cell nucleus. Physiol. Rev. *79*, 683–701.

Park, H.W., Nam, J.H., Kim, J.Y., Namkung, W., Yoon, J.S., Lee, J.S., Kim, K.S., Venglovecz, V., Gray, M.A., Kim, K.H., and Lee, M.G. (2010). Dynamic regulation of CFTR bicarbonate permeability by $[Cl^-]i$ and its role in pancreatic bicarbonate secretion. Gastroenterology *139*, 620–631.

Quinton, P.M. (1999). Physiological basis of cystic fibrosis: a historical perspective. Physiol. Rev. *79*(1, Suppl), S3–S22.

Rennolds, J., Boyaka, P.N., Bellis, S.L., and Cormet-Boyaka, E. (2008). Low temperature induces the delivery of mature and immature CFTR to the plasma membrane. Biochem. Biophys. Res. Commun. *366*, 1025–1029.

Ron, D., and Walter, P. (2007). Signal integration in the endoplasmic reticulum unfolded protein response. Nat. Rev. Mol. Cell Biol. *8*, 519–529.

Roxo-Rosa, M., Xu, Z., Schmidt, A., Neto, M., Cai, Z., Soares, C.M., Sheppard, D.N., and Amaral, M.D. (2006). Revertant mutants G550E and 4RK rescue cystic fibrosis mutants in the first nucleotide-binding domain of CFTR by different mechanisms. Proc. Natl. Acad. Sci. USA *103*, 17891–17896.

Russell, C., and Stagg, S.M. (2010). New insights into the structural mechanisms of the COPII coat. Traffic *11*, 303–310.

Schotman, H., Karhinen, L., and Rabouille, C. (2008). dGRASP-mediated noncanonical integrin secretion is required for Drosophila epithelial remodeling. Dev. Cell *14*, 171–182.

Schröder, M., and Kaufman, R.J. (2005). The mammalian unfolded protein response. Annu. Rev. Biochem. *74*, 739–789.

Shorter, J., Watson, R., Giannakou, M.E., Clarke, M., Warren, G., and Barr, F.A. (1999). GRASP55, a second mammalian GRASP protein involved in the stacking of Golgi cisternae in a cell-free system. EMBO J. *18*, 4949–4960.

Tang, B.L., Gee, H.Y., and Lee, M.G. (2011). The cystic fibrosis transmembrane conductance regulator's expanding SNARE interactome. Traffic *12*, 364–371.

Urano, F., Wang, X., Bertolotti, A., Zhang, Y., Chung, P., Harding, H.P., and Ron, D. (2000). Coupling of stress in the ER to activation of JNK protein kinases by transmembrane protein kinase IRE1. Science *287*, 664–666.

Ward, C.L., Omura, S., and Kopito, R.R. (1995). Degradation of CFTR by the ubiquitin-proteasome pathway. Cell *83*, 121–127.

Wiseman, R.L., Haynes, C.M., and Ron, D. (2010). SnapShot: The unfolded protein response. Cell *140*, 590, e2.

Yoo, J.S., Moyer, B.D., Bannykh, S., Yoo, H.M., Riordan, J.R., and Balch, W.E. (2002). Non-conventional trafficking of the cystic fibrosis transmembrane conductance regulator through the early secretory pathway. J. Biol. Chem. *277*, 11401–11409.

Zeiher, B.G., Eichwald, E., Zabner, J., Smith, J.J., Puga, A.P., McCray, P.B., Jr., Capecchi, M.R., Welsh, M.J., and Thomas, K.R. (1995). A mouse model for the delta F508 allele of cystic fibrosis. J. Clin. Invest. *96*, 2051–2064.

Zhang, K., Wong, H.N., Song, B., Miller, C.N., Scheuner, D., and Kaufman, R.J. (2005). The unfolded protein response sensor IRE1alpha is required at 2 distinct steps in B cell lymphopoiesis. J. Clin. Invest. *115*, 268–281.